Electrochemical CO 2 Reduction to Ethanol with Copper-Based Catalysts

Dilan Karapinar, Charles E Creissen, José Guillermo Rivera de La Cruz, Moritz W Schreiber, Marc Fontecave

Electrochemical CO_2 Reduction to Ethanol with Copper-Based Catalysts

Dilan Karapinar,[1] Charles E. Creissen,[1] Jose Guillermo Rivera de la Cruz,[1] Moritz W. Schreiber,[2] Marc Fontecave[1]*

[1]Laboratoire de Chimie des Processus Biologiques, UMR CNRS 8229, Collège de France-CNRS-Sorbonne Université, PSL Research University, 11 Place Marcelin Berthelot, 75005 Paris, France.

[2] Total Research and Technology, Refining and Chemicals, Division CO_2 Conversion, Feluy, 7181 Seneffe, Belgium

Abstract

Electrochemical CO_2 reduction presents a sustainable route to storage of intermittent renewable energy. Ethanol is an important target product, which is used as fuel additive and as a chemical feedstock. However, electrochemical ethanol production is challenging as it involves the transfer of multiple electrons and protons alongside C−C bond formation. To date, the most commonly employed and effective catalysts are copper-based materials. This review presents and categorizes the most efficient and selective Cu-based electrocatalysts, which are divided into three main groups: oxide-

derived copper, bimetallics, and copper- and nitrogen-doped carbon materials. Only a few other specific examples fall outside this classification. The catalytic performance of these materials for ethanol production in aqueous conditions is discussed in terms of current density, overpotential and faradaic efficiency. A critical evaluation of the factors that contribute to high performance is provided to aid the design of more efficient catalysts for selective ethanol formation.

The electrochemical CO_2 reduction reaction (CO_2RR) enables the conversion of electrical energy into important organic chemical building blocks. Among the different reported CO_2 electroreduction products (typically CO, formic acid, methane, ethylene, ethanol and propanol), ethanol is a notable target molecule. With a worldwide production of ca. 88.5 Mt/y,[1] ethanol is one of the most important organic commodity chemicals. The high energy density and compatibility with existing combustion engines means ethanol is predominantly used as a fuel blend component, but is also a key precursor in the synthesis of various chemical compounds and in the medical and food industries. Currently, ethanol is mainly produced from starch-based biomass (e.g. sugar cane, corn) through fermentation. In recent years, electrochemical CO_2 reduction has gained interest as a potentially more effective and sustainable alternative. Although technically less mature, this route to ethanol production enables the integration of renewably-sourced electricity through either direct (e.g. integrated solar-driven approaches[2]) or indirect (e.g. electrical grid coupling[3]) technologies. The economic feasibility is ultimately dependent on technological advancements that enhance the practicality of this approach.[4, 5] Here, recent developments in electrochemical CO_2 reduction are critically assessed to outline specific catalyst features that have contributed to efficient ethanol production.

The main goal for CO_2 electroreduction to ethanol is to enhance selectivity at high reaction rates. These factors are influenced by the catalyst, the reactor architecture and the process conditions. Systems are most frequently operated in (bulk) neutral or alkaline pH and although alkaline conditions are known to enhance ethylene selectivity from CO_2 reduction, the effects on ethanol production are less explored, therefore differentiation is made within to provide further insight into these effects. Acidic pH

reactions are avoided because of competitive H_2 production through the hydrogen evolution reaction (HER), an undesired side reaction which is favored by elevated concentrations of protons. Alkaline pH conditions generally allow high geometric current densities to be obtained. However, the main disadvantage of alkaline electrolysis is the undesired reaction of CO_2 with OH^- in the electrolyte solution to form carbonate and bicarbonate, which negatively impact the long-term electrolyzer stability and which are much less reactive than CO_2.[6, 7] These effects should be considered, as the total energy input of the complete process will be strongly dependent on losses of this type (e.g. electrolyte regeneration/replacement).

CO_2 electroreduction is operated in either H-cells or flow cell reactors. Reactor architectures in which the CO_2 is diluted in the electrolyte or continuously bubbled around the cathode are termed H-cells and limit CO_2 electroreduction to low specific reaction rates (geometric current densities typically less than 50 mA cm^{-2}) – this is because of CO_2 mass transfer limitations due to the low solubility of CO_2 in aqueous electrolyte solutions (≈ 30 mM). Hence, gas-diffusion electrodes (GDEs), typically implemented in flow cell reactors, are nowadays commonly used to overcome these mass transport limitations and obtain higher geometric current densities (greater than 100 mA cm^{-2}). In this configuration, KOH can be used as the electrolyte and carbonate formation limited with CO_2 flowing from one side of the electrode through the gas diffusion layer (GDL) to react at the catalyst/solution interface at the other side of the electrode. This enables higher current densities to be achieved at respectively lower overpotentials when compared to H-cells.[8-12]

Cu is the foremost metal capable of C-C coupling reactions and hence conversion of CO_2 to products with two or more carbon atoms (C_{2+}).[13, 14] With such Cu-based catalysts, the formation of ethanol competes mainly with ethylene in terms of C_2 products.[15] Numerous efforts have been made to enhance the catalytic activity and selectivity of catalysts towards ethanol. Examples include: varying surface morphology[16-19]; combining different oxidation states of the Cu atoms;[20-24] and modifying the composition of the material[25-29]. Here, we summarize and discuss the state-of-the-art Cu-based catalysts for electrochemical CO_2 reduction into ethanol (Tables 1 and 2). In order to evaluate performance, we have considered the following reported parameters: current density, applied potential and faradaic efficiency (FE). Based on this analysis from the literature, we have identified eighteen catalysts with reported FE above 30% at current densities above −1 mA/cm^2, a threshold that we used in order to discuss the most selective systems. Fourteen of these operated under neutral conditions (Table 1) and six under alkaline conditions (Table 2), two of which were conducted under both conditions. Although CO_2 conversion values are often not provided and experiments were carried out at different current densities, the maximal FE was used for each catalyst, thereby providing meaningful comparison of performance. Additionally, we summarize the few computational studies aimed at understanding how the separation between the ethylene and the ethanol pathways can be tuned. Interestingly, fifteen of the selected systems can be assigned to three classes: oxide-derived Cu, bimetallic Cu-M catalysts, and copper- and N-doped carbon materials – the four remaining systems have specific characteristics that differ from these classifications.

Table 1 – Catalysts for CO_2 electroreduction to ethanol in neutral pH electrolyte solution with FE_{EtOH} > 30%.

Catalyst	Electrolyte	Potential (V *vs.* RHE)	Current Density[b] (mA/cm^2)	Other CO_2RR products[a]	FE_{max} EtOH (%)	Cell type	Time[c] (min)	Ref.
Oxide Derived Copper								
OD Cu/C	0.1 M $KHCO_3$	−0.5	−1	HCOOH, CH_3OH	34.8	H-cell	180	30
Cu sandwich	0.1 M $KHCO_3$	−0.3	−1.25	CO, HCOOH, CH_3OH	31	H-cell	120	31
Cu-Cu_2O-3	0.1 M KCl	−0.4	−7.3	CO, CH_4, CH_3COOH	39.2	H-cell	300	32
Bimetallic								
Ag-Cu_2O_{PB}	0.2 M KCl	−1.2	−3	CO, HCOOH, C_2H_4	34	H-cell	180	33
$Ag_{0.14}/Cu_{0.86}$	1 M $KHCO_3$	−0.84	−300	CO, CH_4, C_2H_4, CH_3COOH	37	Flow cell	20	34
Cu_4Zn	0.1 M $KHCO_3$	−1.05	−28.1	CO, HCOOH, C_2H_4	30	H-cell	60	35
ZnO-CuO	0.1 M $KHCO_3$	−1.15	−31.8	CO, CH_4, C_2H_4, C_3H_7OH	32	H-cell	60	36
Cu_3Au	0.1 M $KHCO_3$	−0.7	−1	CO, HCOOH, CH_3OH	45	H-cell	180	37
Copper- and Nitrogen-Doped Carbon-Based Catalysts								
CuNP/N-doped CNS	0.1 M $KHCO_3$	−1.2	−4.8	CO, CH_4	63	H-cell	60	38
CuNP-N-doped GO	0.1 M $KHCO_3$	−0.25	−4.5	-	56.3	H-cell	n.r.	39
CuNC	0.1 M $CsHCO_3$	−1.2	−16.2	CO	43	H-cell	60	40
Cu/C-0.4	0.1 M $KHCO_3$	−0.7	−1.23	$(CH_3)_2CO$	91	Rotating disk electrode	~65	41

Cu GNC-VL	0.5 M $KHCO_3$	−0.87	−10.4	HCOOH, CH_3OH	70.5	H-cell	60	[42]
Other Copper-Based Catalysts								
Surface modified Cu	0.1 M $KHCO_3$	−1.1	−1.04	HCOOH, C_2H_4, C_3H_7OH	30.6	H-cell	~65	[43]
FeTPP/Cu	0.1 M $KHCO_3$	−0.82	−124	HCOOH, C_2H_4, C_3H_7OH, CH_3COOH	41.2	Flow cell	n.r.	[44]

n.r. not reported, [a] Remaining FE was assigned to H_2, [b] Current density according to the exposed geometric surface area, [c] Duration of the electrolysis which the maximum FE for EtOH was obtained

Oxide Derived Copper: Neutral pH

Recent studies have demonstrated that Cu materials derived from copper oxides (OD Cu) display high activity and selectivity for electroreduction of CO_2 to C_2 products (ethylene and ethanol).[45-48] OD Cu electrodes are generally obtained by growing Cu_2O layers from various Cu-based precursors (e.g. Cu foil, Cu-based MOFs) at high temperature on the surface of the electrode and subsequently reducing this oxide to form Cu^0 sites. The enhanced selectivity for ethanol of such catalysts has been tentatively ascribed to: (i) the presence of residual subsurface oxygen atoms that modify the electronic structure of the surface Cu atoms and increase the CO binding energy, which kinetically favors C–C coupling;[47] (ii) the presence of residual Cu^+ which might work synergistically with adjacent Cu^0 by providing a strong H_2O adsorption site favoring CO_2 conversion to CO;[49, 50] and (iii) morphological features, such as an optimized population of edges and steps as well as a high density of grain boundaries.[17, 22, 49, 51] We note that although oxides and Cu^+ species in some cases were reported to be unstable under reductive reaction conditions,[51-53] there are examples which provide compelling evidence for their stability with specific material modifications.[54-57] Table 1 highlights three different OD Cu systems, showing the highest selectivity for ethanol formation from CO_2RR within this class of catalysts.

Zhao et al. prepared a porous OD Cu/C electrocatalyst, consisting of Cu/Cu_2O particles embedded in a porous carbon matrix, through pyrolysis of a Cu-based metal-organic framework (HKUST-1).[30] First, the MOF was prepared through hydrothermal synthesis using $Cu(NO_3)_2 \cdot 3H_2O$ and benzene-1,3,5-tricarboxylate as precursors. The resulting

MOF was pyrolyzed under an Ar atmosphere at 1000 °C generating the catalyst denoted as OD Cu/C-1000. This catalyst selectively converted CO_2 into ethanol with a maximum FE of 34.8% at a potential of −0.5 V *vs.* RHE in 0.1 M $KHCO_3$, however at a low total current density of −1 mA/cm^2. HCOOH (FE 9.2%) and CH_3OH (FE 13.8%) were also produced from the CO_2RR. Lower activity and selectivity was obtained when pyrolysis was carried out at 900 or 1100 °C. Porous Cu (obtained from a two-step calcination of OD Cu/C-1000 in order to remove carbon species) and porous carbon (obtained from acid treatment of OD Cu/C-1000 in order to remove Cu) electrodes were less active, showing the importance of combining Cu with a porous carbon template. While porous Cu showed lower FE to ethanol and methanol than OD Cu/C-1000 at the same reduction potentials, porous carbon did not show any alcohol production at all.

A 'Cu sandwich' catalyst, composed of a dense array of nanowires, containing a mixture of Cu_2O and CuO on copper foam, exhibited a high FE of 31% for ethanol formation.[31] The material was prepared via a two-step synthesis: (i) Cu_2O oxide layer formation on commercially available copper foam via controlled anodization; and (ii) low temperature annealing (400 °C) resulting in Cu_2O oxidation to CuO and reorganization of the surface into nanowires. The 'Cu sandwich' electrode was able to convert CO_2 to ethanol with a FE of 31% at a very low applied potential of −0.3 V *vs*. RHE however with a quite low but stable current density of −1.25 mA/cm^2. At this potential, HCOOH (FE of 6%), CH_3OH (FE of 14%) and trace amounts of CO were also obtained. Catalysts formed solely through the anodization step ('Cu anodized'; FE= 4-9 %) or annealing step ('Cu annealed'; FE= 16%) proved much less efficient for ethanol production. The high selectivity of the 'Cu sandwich' electrode was tentatively explained by the presence of

an oxide sublayer which prevents the exposed Cu_2O species from being completely reduced, thus providing the surface with a favorable mixture of Cu^+/Cu^{2+} ions with metallic Cu^0. XRD characterization of the 'Cu sandwich' electrode after 18h of electrolysis indeed showed the presence of a Cu_2O layer, which was also the case for the 'Cu annealed' sample but not for 'Cu anodized'. However, no *in situ* analysis was provided, therefore the exact nature of the oxide under reductive potentials is unknown. The greater selectivity of 'Cu sandwich' with respect to 'Cu annealed' was assigned to the observed larger density of composite nanowires, leading to a greater density of active sites. 'Cu sandwich' was also shown to contain a higher concentration of oxygen vacancy defects (determined by electron paramagnetic resonance spectroscopy), which were suggested to promote CO_2 adsorption, stabilize radical intermediate species and thus lower the activation barriers.[58, 59]. However, none of these attributes provided any insight into the ethanol *vs.* ethylene selectivity.

A 3D dendritic Cu-Cu_2O/Cu catalyst was obtained by electrooxidation of a Cu foil anode in the presence of different benzoic acid or pyridinecarboxylic acid derivatives (L) to form Cu^{2+}-L films on a Cu substrate. The resulting electrode was subsequently exposed to cathodic potentials for electroreduction of the Cu^{2+} ions to Cu^0.[32] XPS and XRD analysis confirmed that the film was composed of Cu and Cu_2O. A dendritic structure with a high density of grain boundaries between Cu and Cu_2O, supposed to favor catalytic activity, were observed using scanning and transmission electron microscopy. The best performance towards ethanol production was obtained with the catalyst prepared from the ligand L=1,3,5-benzenetricarboxylic acid (denoted as Cu-Cu_2O-3) – this catalyst reduced CO_2 into ethanol with high FE (39.2%) in 0.1 M KCl, at a low applied potential of

−0.4 V *vs.* RHE with a current density of roughly −10 mA/cm^2. Other products included CO (FE 13.8%), CH_4 (FE 14.2%) and acetic acid (FE of 17.5%). It was assumed that the efficiency of Cu-Cu_2O/Cu came from the high density of exposed active sites and a favorable Cu_2O:Cu ratio.

Bimetallic Systems: Neutral pH

Addition of a secondary metal in copper-based systems is a widely used approach to tune the electronic structure of Cu and the binding energy of the key intermediates of the CO_2RR and thereby improve the activity and selectivity for ethanol.[60, 61] The binding strength of CO, as a key intermediate for ethanol formation, on Cu-based catalysts is related to the d-electron availability, which can be tuned by the introduction of second metal via hybridization of the atomic orbitals.[62, 63] In addition, considering that ethanol requires the initial coupling of two adjacent *CO intermediates on Cu atoms, thus requiring a high local concentration of CO and high coverage of *CO intermediates on the catalyst surface, a CO-generating metal such as Ag, Au or Zn, is most often chosen as a promotor element within M-Cu bimetallics – this is referred to as sequential catalysis. The increased selectivity is often ascribed to a combination of these two effects, with the dominant mechanism being dependent on the length scale of metal mixing. Segregated catalysts are typically influenced more by sequential catalysis whereas alloyed catalysts are more influenced by electronic effects.[64] In Table 1, the five best systems in terms of selectivity for ethanol illustrate the effectiveness of the bimetallic strategy.

Lee et al. prepared Ag-incorporated Cu_2O electrodes through electrochemical co-deposition using either NH_3 or KCN solutions containing Cu and Ag precursors.[33] XRD

characterization of the electrode prepared in KCN (abbreviated as Ag-Cu_2O_{PB}) showed a phase-blended Ag/Cu_2O structure, whereas a phase-separated composition was obtained when the electrode was prepared in NH_3 solution (Ag-Cu_2O_{PS}). EDX analysis of Ag-Cu_2O_{PB} showed a more homogeneous dispersion of Cu and Ag atoms on the surface than for Ag-Cu_2O_{PS}. All the electrode samples had a high atomic Cu content (~66%). Ag-Cu_2O_{PB} displayed selective ethanol formation in KCl with a FE of 34% at a very negative applied potential of −1.2 V *vs.* RHE, representing a high overpotential for such low current density (≈ −3 mA/cm^2).[33] CO (FE 2.3%), C_2H_4 (FE 9.5%) and a trace amount of CH_4 were also formed. The biphasic Cu_2O-Cu catalyst without the Ag dopant showed higher H_2 formation and lower ethanol selectivity (FE 9.7%) at the same applied potential. Instead, ethylene was the major C_2 product, however no clear explanation for the obtained selectivity was provided.

In a recent work, Li. et al. and coworkers prepared several Ag/Cu alloys, with different Ag:Cu ratios, through co-sputtering.[34] The best performances for ethanol formation in 1 M $KHCO_3$ were obtained with a $Ag_{0.14}Cu_{0.86}$ catalyst. High current densities up to −400 mA/cm^2 were achieved in a flow cell reactor configuration using a gas diffusion electrode. The catalyst was deposited on a PTFE substrate, allowing CO_2 gas to diffuse through the PTFE and reach the catalyst-electrolyte solution interface where the CO_2RR takes place. This is one of the rare examples of CO_2 to ethanol conversion in neutral electrolyte using a flow cell system. Under these conditions, the highest FE (37%) for ethanol was obtained at an applied current density of −300 mA/cm^2. C_2H_4 (FE 25%), CH_4 (FE 20%) and acetic acid (FE ≈ 5%) were also produced. It is interesting to note

that under neutral conditions, the performance closely approached that obtained with the same catalyst in 1 M KOH (see below) – this is likely because, under such high current density conditions, the local pH at the catalyst- electrolyte solution interface is expected to become alkaline even in $KHCO_3$.[65] These experiments were complemented with DFT calculations, as discussed in the computational studies section below.

Oxide-derived Cu materials with various amounts of Zn dopant (Cu_xZn) were prepared by Ren et al. through electrodeposition[35]. SEM images showed that the Cu_xZn oxide materials were made of spherical particles (with an average diameter of hundreds of nanometers). In contrast, pure Cu oxides were found in the form of smooth polyhedron particles (with average diameters of 100 nm to 1 μm) and pure Zn oxide films were found in the form of interconnected platelets (with an average diameter of hundreds of nanometers). Selected area electron diffraction (SAED) patterns showed the presence of distinct Cu^0 and Zn^0 crystallites in the Cu_xZn catalysts, indicating phase segregation of Cu and Zn and thus excluding alloys. The study also showed that the concentration of Zn in the Cu_xZn catalyst significantly altered the product distribution. The best performance for ethanol formation (FE = 30% at −1.05 V *vs.* RHE) was achieved with a 4:1 Cu:Zn ratio and the material proved stable for at least 5 h during electrolysis. C_2H_4 (FE 10%) and CO (FE 10%) were also obtained. On pure copper oxide the selectivity to ethylene was roughly two times higher than for ethanol across all studied potentials, while zinc oxide generated no ethylene or ethanol. Zn is thus important for promoting ethanol formation. However, increasing the concentration of Zn above a certain threshold resulted in a decrease of the FE for ethanol, probably because of a too large

decrease of the surface density of active Cu sites, again showing the importance of finding the right balance between the two metals in bimetallic systems.

Similarly, Ren et al. coated the surface of CuO nanowires with ZnO using atomic layer deposition.[36] Such ZnO/CuO materials were then electrochemically pre-reduced to the metallic state CuZn before being used for electrolysis. EDX spectroscopic mapping indicated that the CuO/ZnO layer boundaries had disappeared during reduction and that Cu migrated to the surface. In addition, XRD showed only Cu and Zn phases, with no indication of alloys. The CuZn material catalyzed ethanol formation with a FE of 32% at a very cathodic applied potential of −1.15 V *vs.* RHE. C_2H_4 (FE 7.9%), CO (FE 15.3%) and C_3H_7OH (FE 3.2%) were also produced. Compared to CuZn, the monometallic Cu catalyst produced much lower amounts of ethanol (FE 9.1%). In this study CH_3* was suggested as a possible key intermediate towards ethanol formation, however no DFT calculations were performed. The proposed mechanism involved *CO/*CH_3 coupling, leading to a *$COCH_3$ intermediate which is further reduced to ethanol.

Gold has also been used as a promotor metal. Zhu and coworkers prepared various Cu_xAu_y nanowire arrays (NWAs), with a length of roughly 20 μm and a diameter of roughly 35 to 40 nm, through potentiostatic pulse-electrodeposition using $CuSO_4$ and HAuCl as metal precursors.[37] Different Cu:Au ratios in Cu_xAu_y were obtained by changing the codeposition potential. SAED patterns of the Cu_xAu_y nanowires showed that the materials were polycrystalline and EDS mapping showed that Au and Cu were uniformly spatially distributed. Ethanol formation was maximized on Cu_3Au with the highest FE (48%) obtained at −0.5 V *vs.* RHE in 0.1 M $KHCO_3$. However, at this potential the current density was very small (less than −1 mA/cm^2) and H_2 increased

drastically (up to 60%) with small increase of the overpotential. Since a planar Cu_3Au film with the same crystalline structure did not produce any ethanol under the same conditions, the selectivity of Cu_3Au NWA was attributed to its specific morphology. The authors proposed that the nanowires limit diffusion of both hydroxide and CO to the bulk of the solution, thus increasing the local pH and the concentration of trapped CO thereby favoring C-C coupling. However, while explaining the large FE for C_2 products, this hypothesis did not explain the preference for ethanol.

Copper- and Nitrogen-doped Carbon-based Catalysts: Neutral pH

Porous carbon materials are promising supports due to their excellent electronic conductivity, stability, high surface area and tailorable porosity.[66, 67] Furthermore, high performance for the CO_2RR can be obtained through heteroatom doping (N, P, and S etc.) due to changes in the charge and spin densities of active carbon atoms in the vicinity of the dopants.[68, 69] Nitrogen has been the predominant dopant resulting in novel NC (nitrogen-doped carbon) electrocatalysts. The high electronegativity of nitrogen atoms enables strong polarization of adjacent carbon atoms in the graphitic lattice, while maintaining a high electrical conductivity.[69-73] Several studies reported CO_2 electroreduction into CO[71, 74-76], formate[70, 77] as well as to hydrocarbons[78] and C_2-products[79, 80] catalyzed by NC catalysts. Such materials can be further improved through doping with metallic species (Fe, Ni, Co and Cu), in the form of isolated atoms or metal particles.[81-89] Interestingly, in the specific case of copper doping, this strategy resulted in efficient catalysts for the CO_2RR towards ethanol. To illustrate those achievements, we have highlighted four of the best systems for selective ethanol production from CO_2 electroreduction (Table 1).

Song et al. developed a nanoscale catalyst consisting of copper nanoparticles (CuNP) deposited on a N-doped graphene-like carbon nanospike (CNS) film.[38] CNS was grown on Si wafers through plasma-enhanced chemical vapor deposition (PECVD) in the presence of ammonia (NH_3) at 650°C for 30 min. Copper nanoparticles were electronucleated from $CuSO_4$ solution directly onto the CNS film. The particle size ranged from roughly 30 nm to 100 nm, as determined by SEM and CNS. XPS analysis showed three main types of nitrogen: pyridinic (≈ 25%), pyrrolic (≈ 25%), and graphitic (≈ 40%).[90] Electrochemical experiments showed that CuNP/CNS material catalyzed CO_2 reduction to ethanol with a remarkably high FE (63%), however at a relatively high overpotential (applied potential of −1.2 V *vs.* RHE) and low current density (−2 mA/cm^2). Only CO (FE = 5%) and CH_4 (FE = 5%) were found as other carbon products, H_2 accounting for 10-15%. Neither pure CNS nor Cu nanoparticles supported on glassy carbon electrodes displayed ethanol production at any potential. It was proposed, as supported by DFT calculations discussed below, that the selectivity was due to the synergistic effect of Cu and N-activated C centers, further illustrating the importance of different reactive sites in close proximity for not only favoring C-C coupling but also controlling the ethylene/ethanol selectivity.

A similar study using N-doped graphene oxide (GO) was carried out by Yuan et al.[39] The material ($GOVB_6$) consists of GO, in which the carboxylic groups have been used to covalently attach vitamin B_6 (VB_6 or pyridoxine) as the source of nitrogen.[91] XPS revealed that the material had only pyridinic N atoms with a content of around 2.3%. Cu nanoparticles were chemically deposited on GO-VB_6 through reduction of $Cu(NO_3)_2$ using hydrazine. The materials with different Cu loadings of 5% (GO-VB_6-Cu-1), 10%

(GO-VB_6-Cu-2), 20% (GO-VB_6-Cu-3) and 40% (GO-VB_6-Cu-4) were prepared. The highest FE for ethanol (56.3%) was obtained in 0.1 M $KHCO_3$ at a very low applied potential of −0.25 V *vs.* RHE (current density of approximately −5 mA/cm^2) with GO-VB_6-Cu-2 as the catalyst. XPS and XRD analysis revealed that this catalyst contained metallic copper as well as Cu_2O. A GO-Cu catalyst (no VB6 functionalization) and a GO-VB_6 catalyst (no deposited Cu particles) both displayed lower FEs for ethanol (10.3% and 36.4% respectively) at more cathodic potentials (−0.4 V *vs.* RHE). The good activity and selectivity of this class of materials was proposed to be related to the large electrochemical surface are (ECSA), the enhanced CO_2 adsorption and local CO concentration due to the high concentration of pyridinic N atoms, and low electron transfer resistance. However, the specific role that each of these features play in controlling the ethylene/ethanol separation was not clarified.

Karapinar et al. prepared a CuNC material containing Cu sites in a CuN_4 coordination, atomically dispersed in a N-doped conductive-carbon matrix.[40]. The catalyst was prepared via pyrolysis of a powder mixture of ZIF-8, a Zn(II) zeolitic imidazolate framework, Cu(II) chloride and 1,10-phenanthroline (phen) as a source of N. The mass of $CuCl_2$ was chosen to give 0.5 wt% of Cu in the final material before pyrolysis. The presence of isolated Cu atomic sites in a CuN_4 environment was shown from XANES and EXAFS spectra, which were reminiscent of Cu(II)-phthalocyanine, molecular complexes in which Cu is chelated by four N atoms of the macrocyclic ligand. Furthermore, High Angle Annular Dark Field Transmission Electron Microscopy (HAADF-TEM) showed isolated Cu atoms and the absence of Cu particles, as confirmed by electron energy loss spectroscopy at these sites. XPS analysis revealed the

presence of pyridinic, pyrrolic, graphitic and porphyrin-like N atoms as well of Cu^{2+} and Cu^{+} ions. CuNC reduced CO_2 selectively into ethanol with a maximum FE of 43% at −1.2 V *vs.* RHE in aqueous 0.1M $CsHCO_3$ with an intermediate current density of −16.2 mA/cm^2. Ethanol was the only liquid product and CO (FE 30%) was the only other carbon product. The selectivity of the CO_2RR was dependent on the flow rate of CO_2 (lower flow rates gave higher FE for ethanol) as well the size of the cation, in the order $Li^{+} < Na^{+} < K^{+} < Cs^{+}$, which is likely due to bigger cations serving as better buffering agents and thus increasing the local CO_2 concentration.[92] As a reference material, the copper-free nitrogen-doped carbon material, prepared identically in the absence of copper chloride in the precursor mixture, did not show any ethanol production. *In-situ operando* X-ray Absorption Spectroscopy (XAS) showed that under the cathodic potentials required for CO_2RR to ethanol, the initial isolated Cu sites partially disappeared upon reduction to Cu^{0} and were converted into small Cu clusters, containing no more than 20 atoms, which suggests that these clusters are the catalytically active species. Unexpectedly, as shown by XAS, this transformation is reversible, since upon returning to oxidizing conditions the clusters disappeared and all Cu isolated sites were regenerated – this is likely a consequence of the strong Cu ion chelating ability of the N_4 sites.

A similar study using carbon materials doped with Cu and O (not N) atoms resulted in a catalytic material which was highly selective for ethanol production, confirming the above assumptions about the importance of Cu clusters.[41] Cu bulk metal was dissolved by sonication into molten lithium and the resulting Cu-LiOH was mixed with a carbon support. Leaching of LiOH with water resulted in a carbon material containing isolated

Cu atoms ligated by hydroxyl and carboxyl groups from the carbon surface. Electron microscopy, IR and XAS characterization confirmed the presence of isolated sites. This novel catalyst proved highly selective for ethanol during electrolysis in 0.1 M $KHCO_3$. The highest FE (91%) is the highest value reported so far and was obtained at −0.6/−0.7 V *vs.* RHE. However, this remarkable selectivity was only obtained with low loadings of Cu (< 0.8 wt%) and only in the foot of the catalytic wave, therefore at these potentials only extremely small current densities could be obtained (approximately −1 mA/cm^2). At slightly more negative applied potentials the FE for ethanol dropped and CO and H_2 became the major products. Interestingly, as shown from *in situ* XAS experiments, during electrolysis the atomically dispersed Cu atoms converted to ultrasmall Cu_n clusters, with n= 3 to 4, which were proposed to be the active species, as in the case of CuNC, above. This transformation is reversible since only the isolated atoms could be observed after removing the applied potential.

Zhang et al. prepared a Cu/Cu_2O nanocomposite loaded on the surface of a N-containing carbon material (Cu GNC-VL).[42] For its preparation, a two-dimensional zeolitic imidazolate framework-L (ZIF-L) was vertically grown on graphene oxide (GO). A copper precursor was then introduced into the top mesoporous supporting layer followed by carbonization at 1000 °C for 2 h. XRD analysis and HAADF-TEM images revealed the presence of Cu and Cu_2O nanoparticles. N1s XPS spectra revealed the presence of pyridine-, pyrrole- and graphene-like N atoms. The catalyst exhibited remarkably high selectivity towards ethanol formation reaching FE up to 70.5% at −0.87 V *vs*. RHE, with a moderate current density of −10.4 mA/cm^2. Pyrolyzed ZIF-L in the absence of Cu showed almost ten times lower faradic efficiency for ethanol (FE 8.6%). In addition, as a

reference material, a Cu-ZIF-L@GO material with a different orientation of ZIF-L on GO showed lower ethanol production (FE 40.2%). Cu GNC-VL displayed the highest ECSA of these materials, as determined from double layer capacitance measurements. This work provides an additional illustration of the potential of MOF-derived graphene-based N-doped porous carbon nanocomposites as CO_2RR catalysts.

Other Cu-based Catalysts: Neutral pH

Recent developments in tuning the binding energy of reaction intermediates, local chemical environment, and consequently selectivity have been based on surface modification with molecular adsorbents.[93, 94,95] Recent studies have emphasized that the utilization of additives such as thiols[96-98] amines[97, 99] and pyridinium salts[43, 100-102] is a potential strategy for controlling the CO_2RR selectivity including for maximizing ethanol production. Such molecules provide an opportunity to tune the selectivity via variations of the functional groups that can be synthetically introduced in the additives.[43, 101-103]

Han el al. reported that polycrystalline copper combined with N-substituted aryl pyridinium additives was able to form high yields of ethanol from electrochemical CO_2 reduction.[43] The electrode was an electropolished copper foil working in the presence of pyridinium derivatives in 0.1 M $KHCO_3$. The best FE for ethanol (FE 30.6%) was achieved with 10 mM N-tolylpyridinium chloride at an applied potential of −1.1 V *vs.* RHE. C_2H_4 (FE of 40.5%) was nevertheless the major carbon product, interestingly together with C_3H_7OH (FE of 7.1%). The bare polycrystalline copper electrode showed lower selectivity toward ethanol (FE of 7.2%) in the studied potential range, generating mainly H_2 (FE of 42.8%). The superior activity was shown to be due to the presence of a stable colorless film, derived from reductive dimerization of the N-tolylpyridinium cation, as shown by ^{1}H-NMR spectroscopy and X-ray crystallography, and deposited on the electrode. The activity of the electrode could be tuned by varying the substituents on the N-arylpyridinium compounds suggesting that the steric profile of these additives could play a role in the reactivity of the Cu active sites, resulting in differences in binding to

specific Cu sites and in film packing. In a subsequent study aiming at improving further the selectivity for ethylene and not ethanol via the investigation of a library of organic molecules, Li et al. explained the high selectivity for C_2 products through the effect of the nitrogen atom of the N-aryl-substituted pyridine ring, which stabilized the bound intermediate *CO, thus favoring C-C coupling.[102] This study further supports molecular strategies complementing heterogeneous catalysts for stabilizing intermediates and controlling selectivity through local molecular tuning.

A different rationale, reminiscent of that used for bimetallics (see above), led to the investigation of a molecule-copper composite, FeTPP/Cu, in which an iron-porphyrin, a CO_2 reduction catalyst selective for CO production, serves to generate a high concentration of CO on nearby Cu atoms.[44] The copper electrode was sputtered on a hydrophobic porous polytetrafluoroethylene PTFE substrate and the iron porphyrin was spray-coated on the surface. This indeed was shown to favor not only C-C coupling but also ethanol *vs.* ethylene formation, occurring on Cu atoms. In a flow cell system using 1 M $KHCO_3$, this hybrid catalyst generated ethanol with a FE of 41% at −0.82 V *vs.* RHE at a current density of −124 mA/cm^2.

Table 2 – Catalysts for CO_2 electroreduction to ethanol in alkaline electrolyte solution with $FE_{EtOH} > 30\%$.

Catalyst	Electrolyte	Potential (V *vs.* RHE)	Current Density (mA/cm^2)	Other CO_2RR products[a]	FE_{max} EtOH (%)	Cell type	Time[b] (hour)	Ref.
$Ag_{0.14}/Cu_{0.86}$	1M KOH	−0.67	−250	CO, CH_4, C_2H_4, CH_3COOH	41.4	Flow cell	2	34
ZnO-CuO	1M KOH	−0.69	−200	CO, C_2H_4, C_3H_7OH	41	Flow cell	10	36
N-C/Cu	1M KOH	−0.68	−300	CO, CH_4, C_2H_4, CH_3COOH	52.3	Flow cell	16	104
NGQ/Cu-nr	1M KOH	−0.9	−282.1	C_2H_4, C_3H_7OH	≈ 45	Flow cell	100	105
$Ce(OH)_x/Cu$	1M KOH	−0.7	−300	C_2H_4, CH_3COOH	42.6	Flow cell	6	106
GB-Cu	1M KOH	−1.3	−45	CO, CH_4, C_2H_4	31.7	Flow cell	n.r.	107

n.r. not reported, [a] remaining FE was assigned to H_2, [b] Duration of the electrolysis which the maximum FE for EtOH was obtained.

Recent implementation of gas diffusion electrodes (GDEs) in gas-fed flow cells has enabled the use of alkaline electrolytes.[108] We briefly here describe the few systems that have led to relatively high selectivity for ethanol. The comparison suggests that alkaline conditions do not specifically favor ethanol production over neutral conditions, since the highest reported faradaic efficiencies are roughly 40-50% (Table 2).

Bimetallic Systems: Alkaline pH

One clear comparison between alkaline and neutral conditions comes from the investigation of the $Ag_{0.14}Cu_{0.86}$ catalyst described in a previous section. This material was studied in both 1 M $KHCO_3$ and 1 M KOH under similar flow conditions using a GDE.[34] Comparable FE values for ethanol were obtained (37 *vs.* 41 %) at similar current densities. This could in part be related to the similar local environment expected for both conditions, where the pH is known to rise significantly with such high current density.[109, 110]

D. Ren and collaborators draw a similar conclusion from the CuZn catalyst they developed.[36] This catalyst was prepared through electroreduction of a bimetallic oxide consisting of CuO nanowires coated with ZnO through atomic layer deposition. During electroreduction Cu atoms migrate to the surface to yield 6% surface atomic percentage and the boundary between the CuO and ZnO layers disappear. Only Cu and Zn/ZnO phases were present with no evidence for a CuZn alloy. This catalyst was studied in a H-cell with a $KHCO_3$ electrolyte as well as in a flow cell, allowing CO_2 gas to diffuse through the GDE towards the catalyst/electrolyte interface with a KOH electrolyte. Although the flow cell setup provided much higher current densities (−200 *vs.* −10

mA/cm^2) at lower applied potentials, maximum FEs for ethanol were comparable (40% *vs.* 32%).

Copper- and Nitrogen-doped Carbon-based Catalysts: Alkaline pH

The following studies follow the rationale discussed above: that the combination of Cu with N-doped carbon (NC) provides selective catalysts for ethanol. Wang and collaborators developed a highly selective NC/Cu catalyst for ethanol.[104] The NC/Cu catalyst was fabricated through sequential sputter deposition of Cu nanoparticles and NC on the surface of a PTFE membrane. The highest FE for ethanol (52%) was obtained at a current density of −300 mA/cm^2 at −0.68 V *vs.* RHE. It was also found that the selectivity was significantly dependent on the atomic percentage of nitrogen in the NC layer, likely due to the different electron-donating abilities of such layers. The most efficient catalyst contained roughly 34% nitrogen and the highest amount of pyridinic N, which is the most electron-donating species as it has a lone pair of electrons in the plane of the carbon matrix.

A similar approach adopted by Chen et al. combined N-doped graphene quantum dots (NGQs) with Cu. NGQs were obtained by N-doping of graphene oxide and were blended with CuO nanorods (CuO-nr) obtained through calcination of $Cu(OH)_2$.[105] The catalyst precursor was deposited on PTFE and the active NGQ/Cu-nr catalyst was formed *in situ* by electroreduction of CuO. This stable catalyst enabled more selective ethanol production than a Cu-nr catalyst which lacked the NGQ component, (42% *vs.* 15%), with a current density of −282 mA/cm^2 at −0.9 V *vs.* RHE. The performances of NGQ/Cu-nr

were not assigned to increased active surface area or higher local CO concentration but rather to the synergistic effect of NGQ and Cu-nr. This conclusion was based on DFT calculations, as discussed below.

Other Examples: Alkaline pH

Very recently, introduction of a stable metal oxide was shown to improve the selectivity of Cu for ethanol.[106] This was based on the rationale that oxides promote water dissociation into hydroxide and an adsorbed *H atom.[111] This is expected to favor ethanol formation, since H_2O stimulates ethylene formation while increased *H coverage stimulates ethanol through hydrogenation.[112, 113] In one example, $Ce(OH)_x$ was electrodeposited on a Cu-sputtered PTFE substrate to generate a GDE. This $Ce(OH)_x$/Cu catalyst proved stable and more selective for ethanol than the undoped Cu material with a FE of 43% (as compared to 29%) at a current density of −300 mA/cm^2 and an increased ethanol/ethylene ratio. Cerium oxide proved superior to other oxides (Ga, Mn, Zr, Ti).

Chen et al. used poly-vinylpyrrolidone (PVP) as an additive to introduce a high density of grain boundaries into metallic copper during electrodeposition. The GDE-deposited catalyst exhibited relatively high selectivity for ethanol (FE 31.7%) and a high ethanol-to-ethylene ratio, when compared with metallic Cu deposited in the absence of PVP.[107] This result further supported the idea that the density of grain boundaries is an important parameter with respect to controlling the product selectivity of the CO_2RR.[114, 115]

Computational studies

While extensive DFT calculations have provided valuable insights into the C-C coupling step leading to C_2 products, ethylene and ethanol, as well as into the possible intermediates, they failed to explain the bifurcation between the ethylene and the ethanol pathways.[15] This is unfortunate since ethylene is in general the major C_2 product during CO_2 electroreduction catalyzed by Cu-based materials and a better understanding of how this bifurcation is controlled would help in designing more selective catalysts for ethanol.

Briefly, computational studies have well established that the major mechanism for C−C coupling involves two adjacent adsorbed *CO molecules, therefore C_1 *vs.* C_2 selectivity greatly depends on the coverage of surface *CO intermediate. It is worth mentioning that some calculations invoke more reduced C_1 intermediates, such as $*CH_2$, leading to C_2 intermediates via $*CO-*CH_2$ coupling.[15] However, these mechanisms are less likely to operate as their kinetics are less favorable due to the much lower surface density of such C_1 intermediates as compared to *CO. Accordingly, recent time-resolved monitoring of intermediates on Cu surface (*CO, *CHO and *OCCO) have shown that the hydrogenation of *CO and its dimerization are kinetically independent and that the former has slower kinetics so C-C coupling occurs without the participation of *CHO.[116] After the C−C coupling step, several reduction steps involving one electron, one proton and the loss of one of the two oxygen atoms, generates a series of C_2 intermediates, which have been proposed to proceed either through loss of the last oxygen atom towards ethylene or via hydrogenation towards ethanol. Two intermediates, either $*C_2H_2O$ or $*C_2H_3O$ shown in Figure 1, are most often proposed as the main points of

bifurcation between the ethylene and ethanol pathways. A recent significant computational work established that the C-C coupling energy decreased with increased CO coverage on Cu (111) surface, due to increased adsorbate-adsorbate interaction. But more interestingly, calculations showed that the reaction energy associated with the conversion of $*C_2H_2O$ into $*C_2H_3O$ towards ethanol also decreased as a function of *CO coverage more than that associated with the formation of *CCH towards ethylene.[44] These calculations pointed out for the first time the importance of high *CO coverage as for steering selectivity from ethylene to ethanol and validated the approaches based on combinations of Cu with a component selectively active for CO_2 reduction to CO.

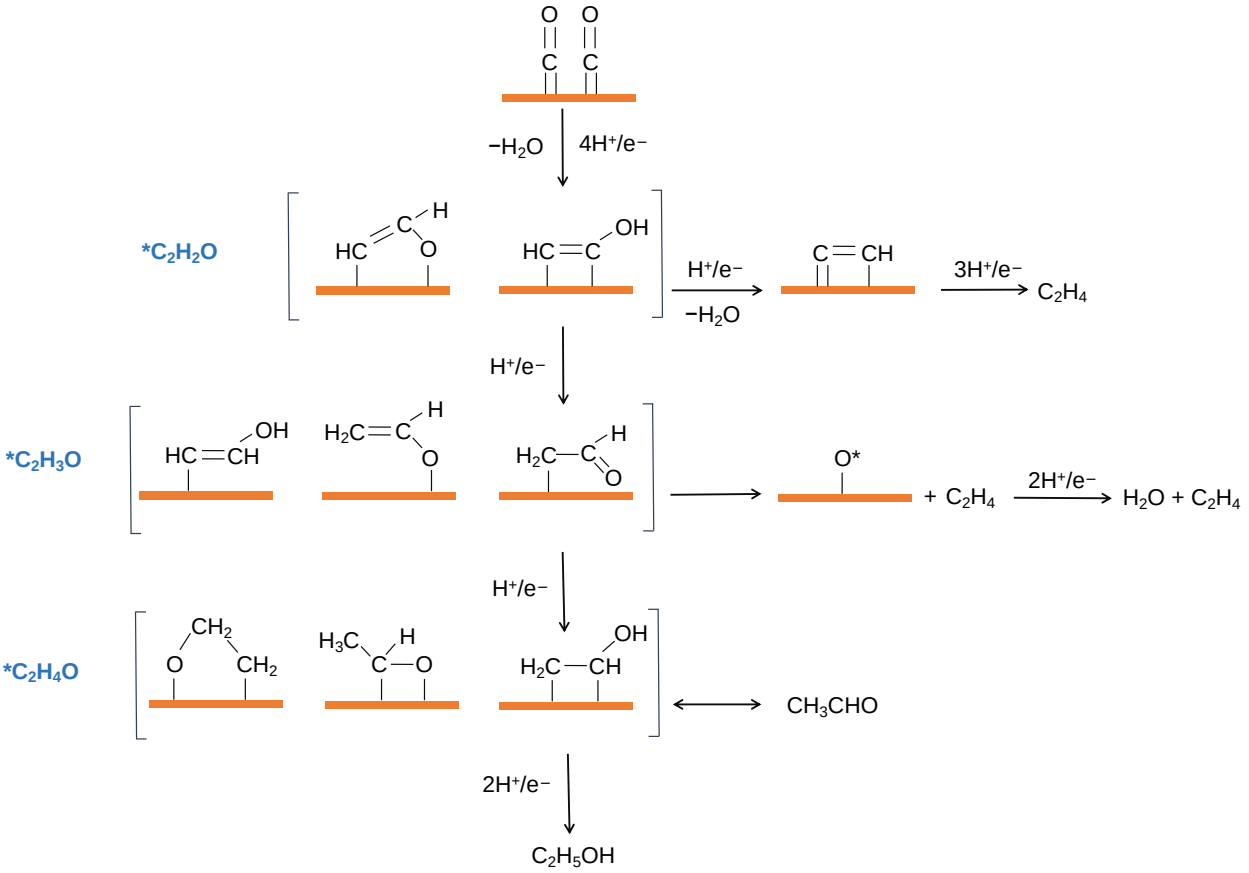

Figure 1: Possible mechanistic pathways of CO_2 reduction to C_2H_4 and C_2H_5OH.[15]

Within the studies presented in Tables 1 and 2, most of them provided only hypotheses and speculations regarding the selectivity of the specific catalyst under investigation. Very few included parallel theoretical characterization. Furthermore, most of these calculations, while establishing favourable pathways towards C_2 *vs.* C_1 products, provide a vague explanation for the larger selectivities for ethanol. Here we briefly discuss the outcomes of the most relevant studies.[34, 38, 104-106, 117]

The specific reactivity of oxide-derived copper materials is often assigned to the presence of subsurface oxygen atoms and residual copper ions.[47] However, certain studies have shown that the stability of either species is limited under the very reducing reaction conditions and therefore the presence of oxides and/or Cu^+ is highly dependent on the catalyst being used.[54-57] Nonetheless, there is an agreement that undercoordinated sites located at grain boundaries are active catalytic sites. As discussed above, grain boundary-rich Cu materials generate high yields of ethanol from CO_2 reduction.[107]

On this basis, Piqué et al. modeled square four-atom Cu islands on Cu(100) facets on which CO reduction showed a clear preference for ethanol formation *vs.* ethylene formation, as compared to Cu(100) facets.[117] In this study, the key intermediate from which the ethanol and ethylene pathways bifurcate is $*C_2H_3O$ (Figure 1). Based on the analysis of the energetics of the proton-electron transfer to $*C_2H_3O$, it appears that the ethanol preference can be modulated by 3 factors: (i) the O* adsorption energy; or (ii) the adsorption energy of acetaldehyde, $*C_2H_4O$ (Figure 1). Specifically, the binding of

*C_2H_4O on this model of undercoordinated sites at grain boundaries is much stronger than that of *O, explaining the preference for ethanol formation.

With respect to bimetallics, the $Ag_{0.14}Cu_{0.86}$ system was studied computationally.[33] In contrast to the previous studies, the branching intermediate in that case was *C_2H_2O. Here, DFT calculations on both Cu(111) and Ag-doped Cu(111) showed that the presence of Ag has a stabilizing effect almost exclusively on the next intermediate, *C_2H_3O, in the ethanol pathway, making it more energetically favorable than the ethylene pathway.

Two computational studies addressed the ethanol selectivity of Cu catalysts associated with nitrogen doped carbon materials, N-C/Cu and NGQ/Cu-nr in Table 2. In the case of N-C/Cu, the catalyst was modelled as a N-C (N-doped graphene) layer above a Cu surface with the reaction taking place in the space between the two layers.[104] Here, the branching intermediate is *C_2H_2O, Figure 1. Calculations of the reaction energies showed that the ethanol selectivity was facilitated only when the graphene layer was doped with N, while with undoped graphene layer or in the absence of graphene, ethylene was favored. Due to N atoms in the N-C layer, the C-O bond in *C_2H_2O was stabilized, the stabilizing effect dependent on the distance between the NG and the Cu planes. In the second study,[105] the branching intermediate is *C_2H_3O. The Cu(111) surface was selected as the model of Cu and a layer of N-doped graphene (NG) covered the surface, giving the NG/Cu model, in which the reaction takes place at the top of the surface. While, as expected, the calculations showed a preference for ethylene in the case of a Cu surface without the NG layer, the ethanol pathway was more favorable on NG/Cu. It was specifically shown that in the case of NG/Cu, the more

stable *C_2H_3O intermediate had its O atom attached to the NG layer resulting in the stabilization of the C-O bond. This is caused by the uplift and the lower occupation of the antibonding state.[118] As a consequence, the subsequent proton-electron transfer to generate *C_2H_4O, towards ethanol production, had a free energy barrier lower than that of ethylene formation.

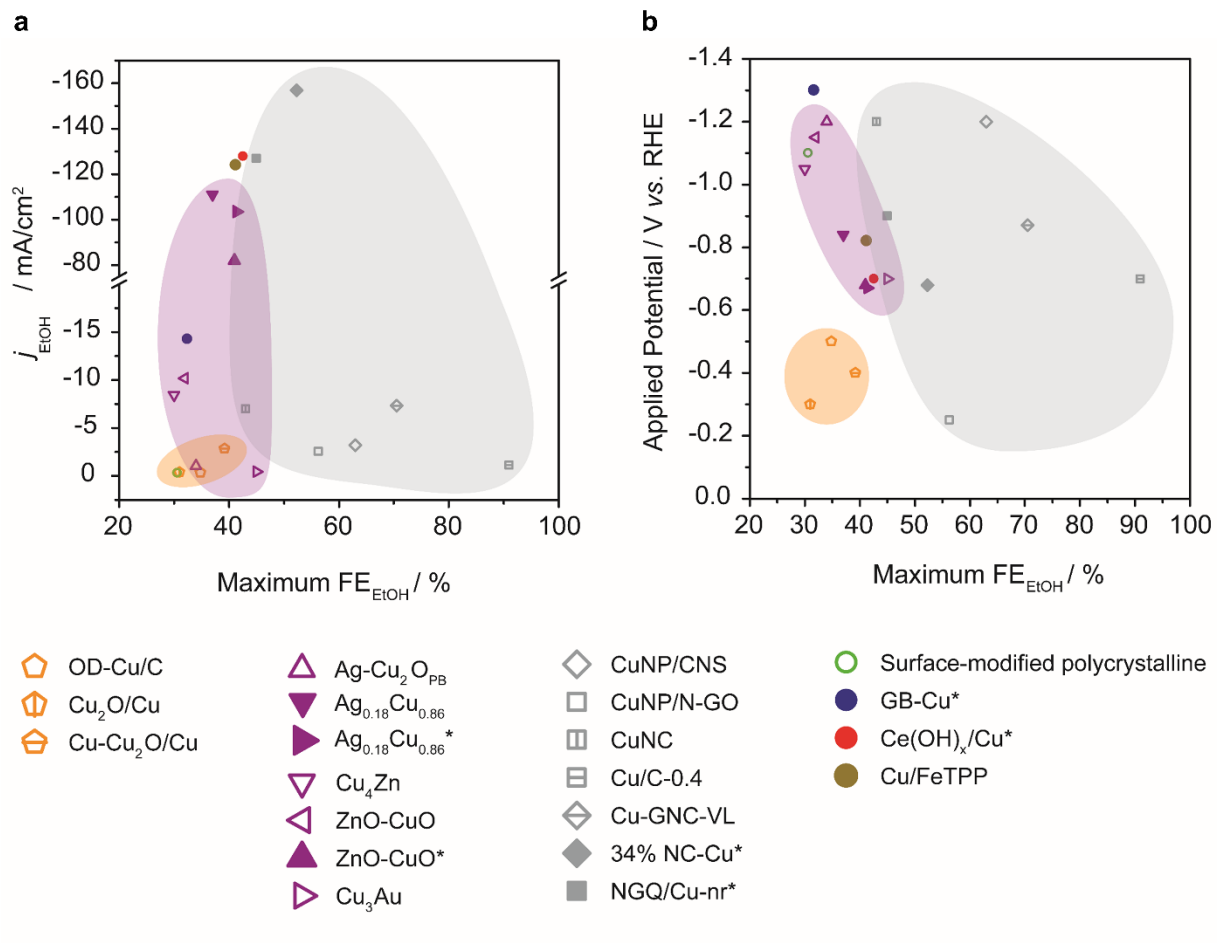

Figure 2: Electrocatalysts exhibiting a FE_{max} ≥ 30% for CO_2-to-Ethanol conversion: a) Partial current density of ethanol production (j_{EtOH}) versus maximum FE for ethanol production, b) The applied potential at which FE_{max} is achieved maximum versus FE for ethanol production. Different catalyst families are highlighted with colored clouds and symbols: oxide-derived Cu (orange); bimetallics (purple); NC-Cu (grey). All H-cell conditions are represented with empty symbols, flow cell conditions with filled symbols, and those operated in KOH with an asterisk (*).

Summary and Outlook

Among the nineteen best Cu-based catalysts for CO_2 electroreduction to ethanol, fifteen belong to three classes: oxide-derived Cu, Cu-M bimetallics and Cu-doped carbon materials, with the four others having very specific characteristics which place them outside the aforementioned classification. Figure 2 shows an overview of the performance of the aforementioned catalysts for electrochemical CO_2 reduction into ethanol with $FE_{max} \geq 30\%$. The plots have been selected to allow a direct comparison of the different catalysts in terms of selectivity (FE_{max} values) and activity (partial current density for ethanol, obtained by multiplying the total geometric current density by FE_{max} for ethanol) (Figure 2a), as well as in terms of the applied potential required to achieve FE_{max} (Figure 2b).

Analysis of these data show the following trends:

- The selectivity for ethanol increases in the order: oxide-derived Cu (FE_{max} 30-40%) ≈ bimetallics (30-45%) < Cu-doped Carbon (45-90%) (Figure 2a)
- Regarding the most selective Cu-doped Carbon systems, the largest FE_{max} values were obtained in H-cells at very low current densities (j_{EtOH} = −1 to −7 mA/cm^2) while at the largest current densities in flow cells (j_{EtOH}= −120 to −150 mA/cm^2) FE_{max} values were below 52%. Furthermore, the largest FE_{max} values were generally obtained at quite negative applied potentials (−0.7 to −1.3 V *vs.* RHE), with the only exception being CuNP-Ndoped-GO (−0.25 V *vs.* RHE). The oxide-derived Cu systems catalyze ethanol formation at significantly lower applied potentials (−0.3 to −0.5 V *vs.* RHE) but unfortunately with very low current densities. The bimetallic

systems function at much higher potentials (−0.7 to −1.2 V *vs.* RHE) however with larger current densities (j_{EtOH} = −10 to −110 mA/cm^2) than the oxide-derived Cu.

- GDEs under flow conditions in KOH generate very high current densities (j_{EtOH} = −80 to −160 mA/cm^2). However, they do not provide significant improvement in selectivity for ethanol (FE_{max} ≈ 40-50%). For example, ZnO−CuO gave a FE_{EtOH} of 41% in a flow cell in KOH, compared with 32% in a H-cell in $KHCO_3$. Again, the best catalyst was NC−Cu, a member of the Cu-doped carbon family with FE_{max} of 52% and j_{EtOH} of −160 mA/cm^2.
- Outside of the three classes, both the $Ce(OH)_x$/Cu and Fe(TPP)/Cu catalysts, studied in flow conditions, compare well with the other systems studied under similar conditions, with high current density (j_{EtOH} = −120 to −130 mA/cm^2) and FE_{max} ≈ 40%.

From the collation and analysis of reported systems for ethanol production, it can be seen that while the level of current density is a matter of device design and experimental conditions the ethanol *vs.* ethylene selectivity is more a matter of catalyst, with large differences between the classes of catalysts.

Care must be taken in differentiating between the systems studied in H-cells and flow cells, and between flow cells operated in neutral or alkaline conditions. In fact, only two systems among the nineteen catalysts have been studied in two different conditions. $Ag_{0.14}Cu_{0.86}$ was studied only in a flow cell using either $KHCO_3$ or KOH electrolyte, without any significant differences in terms of performances, which as mentioned could be due to the similarly high local pH observed in carbonate buffers under high current density operation. ZnO−CuO was studied either in a H-cell using $KHCO_3$ or in a flow cell using KOH, leading to large differences in terms of current density but with a lower

applied potential required to reach FE_{max} in KOH – this highlights the important role that device design plays in overall performance, where mass transport is less limited in the flow cell enabling higher currents to be achieved. However, this does not play a significant role in selectivity towards ethanol.

The trends we have observed in performance identify carbon-based materials doped with copper and heteroatoms such as nitrogen, as frontrunners. The highest selectivity towards ethanol production, irrespective of operating conditions, arises from this class of materials making them a notable target for future research. However, there is still a substantial amount of effort required to improve the integration of such catalysts in flow cells, which would allow them to selectively generate ethanol at high current densities. Ultimately, a combination of experimental, analytical (both *in situ* and *ex situ*), and computational results will provide the mechanistic insights required to systematically design carbon-based Cu catalysts for enhanced CO_2 electroreduction to ethanol.

TOC Image

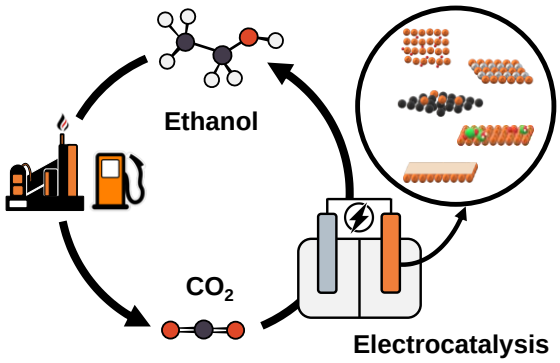

References

1. Renewable fuels Association.2020 Ethanol Industry Outlook, Washington, DC, 2020.
2. Creissen, C. E.; Fontecave, M., Solar Driven Electrochemical CO_2 Reduction with Heterogeneous Catalysts. *Advanced Energy Materials* **2020**, 2002652.
3. De Luna, P.; Hahn, C.; Higgins, D.; Jaffer, S. A.; Jaramillo, T. F.; Sargent, E. H., What would it take for renewably powered electrosynthesis to displace petrochemical processes? *Science* **2019,** *364* (6438), eaav3506.
4. Bushuyev, O. S.; De Luna, P.; Dinh, C. T.; Tao, L.; Saur, G.; van de Lagemaat, J.; Kelley, S. O.; Sargent, E. H., What Should We Make with CO_2 and How Can We Make It? *Joule* **2018,** *2* (5), 825-832.
5. Jouny, M.; Luc, W.; Jiao, F., Correction to "General Techno-Economic Analysis of CO_2 Electrolysis Systems". *Industrial & Engineering Chemistry Research* **2020,** *59* (16), 8121-8123.
6. Schulz, K. G.; Riebesell, U.; Rost, B.; Thoms, S.; Zeebe, R. E., Determination of the rate constants for the carbon dioxide to bicarbonate inter-conversion in pH-buffered seawater systems. *Marine Chemistry* **2006,** *100* (1), 53-65.
7. König, M.; Vaes, J.; Klemm, E.; Pant, D., Solvents and Supporting Electrolytes in the Electrocatalytic Reduction of CO_2. *iScience* **2019,** *19*, 135-160.
8. Dinh, C. T.; Burdyny, T.; Kibria, M. G.; Seifitokaldani, A.; Gabardo, C. M.; Garcia de Arquer, F. P.; Kiani, A.; Edwards, J. P.; De Luna, P.; Bushuyev, O. S.; Zou, C.; Quintero-Bermudez, R.; Pang, Y.; Sinton, D.; Sargent, E. H., CO_2 electroreduction to ethylene via hydroxide-mediated copper catalysis at an abrupt interface. *Science* **2018,** *360* (6390), 783-787.
9. Dinh, C.-T.; García de Arquer, F. P.; Sinton, D.; Sargent, E. H., High Rate, Selective, and Stable Electroreduction of CO_2 to CO in Basic and Neutral Media. *ACS Energy Letters* **2018,** *3* (11), 2835-2840.
10. Gabardo, C. M.; Seifitokaldani, A.; Edwards, J. P.; Dinh, C.-T.; Burdyny, T.; Kibria, M. G.; O'Brien, C. P.; Sargent, E. H.; Sinton, D., Combined high alkalinity and pressurization enable efficient CO_2 electroreduction to CO. *Energy & Environmental Science* **2018,** *11* (9), 2531-2539.
11. Kibria, M. G.; Dinh, C.-T.; Seifitokaldani, A.; De Luna, P.; Burdyny, T.; Quintero-Bermudez, R.; Ross, M. B.; Bushuyev, O. S.; García de Arquer, F. P.; Yang, P.; Sinton, D.; Sargent, E. H., A Surface Reconstruction Route to High Productivity and Selectivity in CO_2 Electroreduction toward C_{2+} Hydrocarbons. *Advanced Materials* **2018,** *30* (49), 1804867.
12. Garcia de Arquer, F. P.; Dinh, C. T.; Ozden, A.; Wicks, J.; McCallum, C.; Kirmani, A. R.; Nam, D. H.; Gabardo, C.; Seifitokaldani, A.; Wang, X.; Li, Y. C.; Li, F.; Edwards, J.; Richter, L. J.; Thorpe, S. J.; Sinton, D.; Sargent, E. H., CO_2 electrolysis to multicarbon products at activities greater than 1 A cm(-2). *Science* **2020,** *367* (6478), 661-666.

13. Nitopi, S.; Bertheussen, E.; Scott, S. B.; Liu, X.; Engstfeld, A. K.; Horch, S.; Seger, B.; Stephens, I. E. L.; Chan, K.; Hahn, C.; Nørskov, J. K.; Jaramillo, T. F.; Chorkendorff, I., Progress and Perspectives of Electrochemical CO_2 Reduction on Copper in Aqueous Electrolyte. *Chemical Reviews* **2019,** *119* (12), 7610-7672.
14. Gao, D.; Arán-Ais, R. M.; Jeon, H. S.; Roldan Cuenya, B., Rational catalyst and electrolyte design for CO_2 electroreduction towards multicarbon products. *Nature Catalysis* **2019,** *2* (3), 198-210.
15. Todorova, T. K.; Schreiber, M. W.; Fontecave, M., Mechanistic Understanding of CO_2 Reduction Reaction (CO_2RR) Toward Multicarbon Products by Heterogeneous Copper-Based Catalysts. *ACS Catalysis* **2020,** *10* (3), 1754-1768.
16. Tang, W.; Peterson, A. A.; Varela, A. S.; Jovanov, Z. P.; Bech, L.; Durand, W. J.; Dahl, S.; Nørskov, J. K.; Chorkendorff, I., The importance of surface morphology in controlling the selectivity of polycrystalline copper for CO_2 electroreduction. *Physical Chemistry Chemical Physics* **2012,** *14* (1), 76-81.
17. Ren, D.; Wong, N. T.; Handoko, A. D.; Huang, Y.; Yeo, B. S., Mechanistic Insights into the Enhanced Activity and Stability of Agglomerated Cu Nanocrystals for the Electrochemical Reduction of Carbon Dioxide to n-Propanol. *The Journal of Physical Chemistry Letters* **2016,** *7* (1), 20-24.
18. Reller, C.; Krause, R.; Volkova, E.; Schmid, B.; Neubauer, S.; Rucki, A.; Schuster, M.; Schmid, G., Selective Electroreduction of CO_2 toward Ethylene on Nano Dendritic Copper Catalysts at High Current Density. *Advanced Energy Materials* **2017,** *7* (12), 1602114.
19. Huan, T. N.; Simon, P.; Rousse, G.; Genois, I.; Artero, V.; Fontecave, M., Porous dendritic copper: an electrocatalyst for highly selective CO_2 reduction to formate in water/ionic liquid electrolyte. *Chem Sci* **2017,** *8* (1), 742-747.
20. Frese, K. W., Electrochemical Reduction of CO_2 at Intentionally Oxidized Copper Electrodes. *Journal of The Electrochemical Society* **1991,** *138* (11), 3338-3344.
21. Le, M.; Ren, M.; Zhang, Z.; Sprunger, P. T.; Kurtz, R. L.; Flake, J. C., Electrochemical Reduction of CO_2 to CH_3OH at Copper Oxide Surfaces. *Journal of The Electrochemical Society* **2011,** *158* (5), E45-E49.
22. Li, C. W.; Ciston, J.; Kanan, M. W., Electroreduction of carbon monoxide to liquid fuel on oxide-derived nanocrystalline copper. *Nature* **2014,** *508*, 504.
23. Dutta, A.; Rahaman, M.; Luedi, N. C.; Mohos, M.; Broekmann, P., Morphology Matters: Tuning the Product Distribution of CO_2 Electroreduction on Oxide-Derived Cu Foam Catalysts. *ACS Catalysis* **2016,** *6* (6), 3804-3814.
24. Rahaman, M.; Dutta, A.; Zanetti, A.; Broekmann, P., Electrochemical Reduction of CO_2 into Multicarbon Alcohols on Activated Cu Mesh Catalysts: An Identical Location (IL) Study. *ACS Catalysis* **2017,** *7* (11), 7946-7956.
25. Kim, D.; Resasco, J.; Yu, Y.; Asiri, A. M.; Yang, P., Synergistic geometric and electronic effects for electrochemical reduction of carbon dioxide using gold-copper bimetallic nanoparticles. *Nat Commun* **2014,** *5*, 4948.
26. Ma, S.; Sadakiyo, M.; Heima, M.; Luo, R.; Haasch, R. T.; Gold, J. I.; Yamauchi, M.; Kenis, P. J. A., Electroreduction of Carbon Dioxide to Hydrocarbons Using Bimetallic Cu–Pd Catalysts with Different Mixing Patterns. *Journal of the American Chemical Society* **2017,** *139* (1), 47-50.
27. Li, Q.; Fu, J.; Zhu, W.; Chen, Z.; Shen, B.; Wu, L.; Xi, Z.; Wang, T.; Lu, G.; Zhu, J.-j.; Sun, S., Tuning Sn-Catalysis for Electrochemical Reduction of CO_2 to CO via

the Core/Shell Cu/SnO_2 Structure. *Journal of the American Chemical Society* **2017,** *139* (12), 4290-4293.
28. Kim, D.; Xie, C.; Becknell, N.; Yu, Y.; Karamad, M.; Chan, K.; Crumlin, E. J.; Nørskov, J. K.; Yang, P., Electrochemical Activation of CO_2 through Atomic Ordering Transformations of AuCu Nanoparticles. *Journal of the American Chemical Society* **2017,** *139* (24), 8329-8336.
29. Dai, L.; Qin, Q.; Wang, P.; Zhao, X.; Hu, C.; Liu, P.; Qin, R.; Chen, M.; Ou, D.; Xu, C.; Mo, S.; Wu, B.; Fu, G.; Zhang, P.; Zheng, N., Ultrastable atomic copper nanosheets for selective electrochemical reduction of carbon dioxide. *Science Advances* **2017,** *3* (9), e1701069.
30. Zhao, K.; Liu, Y.; Quan, X.; Chen, S.; Yu, H., CO_2 Electroreduction at Low Overpotential on Oxide-Derived Cu/Carbons Fabricated from Metal Organic Framework. *ACS Applied Materials & Interfaces* **2017,** *9* (6), 5302-5311.
31. Daiyan, R.; Saputera, W. H.; Zhang, Q.; Lovell, E.; Lim, S.; Ng, Y. H.; Lu, X.; Amal, R., 3D Heterostructured Copper Electrode for Conversion of Carbon Dioxide to Alcohols at Low Overpotentials. *Advanced Sustainable Systems* **2019,** *3* (1), 1800064.
32. Zhu, Q.; Sun, X.; Yang, D.; Ma, J.; Kang, X.; Zheng, L.; Zhang, J.; Wu, Z.; Han, B., Carbon dioxide electroreduction to C_2 products over copper-cuprous oxide derived from electrosynthesized copper complex. *Nature Communications* **2019,** *10* (1), 3851.
33. Lee, S.; Park, G.; Lee, J., Importance of Ag–Cu Biphasic Boundaries for Selective Electrochemical Reduction of CO_2 to Ethanol. *ACS Catalysis* **2017,** *7* (12), 8594-8604.
34. Li, Y. C.; Wang, Z.; Yuan, T.; Nam, D.-H.; Luo, M.; Wicks, J.; Chen, B.; Li, J.; Li, F.; de Arquer, F. P. G.; Wang, Y.; Dinh, C.-T.; Voznyy, O.; Sinton, D.; Sargent, E. H., Binding Site Diversity Promotes CO_2 Electroreduction to Ethanol. *Journal of the American Chemical Society* **2019,** *141* (21), 8584-8591.
35. Ren, D.; Ang, B. S.-H.; Yeo, B. S., Tuning the Selectivity of Carbon Dioxide Electroreduction toward Ethanol on Oxide-Derived Cu_xZn Catalysts. *ACS Catalysis* **2016,** *6* (12), 8239-8247.
36. Ren, D.; Gao, J.; Pan, L.; Wang, Z.; Luo, J.; Zakeeruddin, S. M.; Hagfeldt, A.; Grätzel, M., Atomic Layer Deposition of ZnO on CuO Enables Selective and Efficient Electroreduction of Carbon Dioxide to Liquid Fuels. *Angewandte Chemie International Edition* **2019,** *58* (42), 15036-15040.
37. Zhu, W.; Zhao, K.; Liu, S.; Liu, M.; Peng, F.; An, P.; Qin, B.; Zhou, H.; Li, H.; He, Z., Low-overpotential selective reduction of CO_2 to ethanol on electrodeposited CuxAuy nanowire arrays. *Journal of Energy Chemistry* **2019,** *37*, 176-182.
38. Song, Y.; Peng, R.; Hensley, D. K.; Bonnesen, P. V.; Liang, L.; Wu, Z.; Meyer III, H. M.; Chi, M.; Ma, C.; Sumpter, B. G.; Rondinone, A. J., High-Selectivity Electrochemical Conversion of CO_2 to Ethanol using a Copper Nanoparticle/N-Doped Graphene Electrode. *ChemistrySelect* **2016,** *1* (19), 6055-6061.
39. Yuan, J.; Yang, M.-P.; Zhi, W.-Y.; Wang, H.; Wang, H.; Lu, J.-X., Efficient electrochemical reduction of CO_2 to ethanol on Cu nanoparticles decorated on N-doped graphene oxide catalysts. *Journal of CO_2 Utilization* **2019,** *33*, 452-460.
40. Karapinar, D.; Huan, N. T.; Ranjbar Sahraie, N.; Li, J.; Wakerley, D.; Touati, N.; Zanna, S.; Taverna, D.; Galvão Tizei, L. H.; Zitolo, A.; Jaouen, F.; Mougel, V.; Fontecave, M., Electroreduction of CO_2 on Single-Site Copper-Nitrogen-Doped Carbon

Material: Selective Formation of Ethanol and Reversible Restructuration of the Metal Sites. *Angewandte Chemie International Edition* **2019,** *58* (42), 15098-15103.
41. Xu, H.; Rebollar, D.; He, H.; Chong, L.; Liu, Y.; Liu, C.; Sun, C.-J.; Li, T.; Muntean, J. V.; Winans, R. E.; Liu, D.-J.; Xu, T., Highly selective electrocatalytic CO_2 reduction to ethanol by metallic clusters dynamically formed from atomically dispersed copper. *Nature Energy* **2020,** *5* (8), 623-632.
42. Zhang, Y.; Li, K.; Chen, M.; Wang, J.; Liu, J.; Zhang, Y., Cu/Cu2O Nanoparticles Supported on Vertically ZIF-L-Coated Nitrogen-Doped Graphene Nanosheets for Electroreduction of CO_2 to Ethanol. *ACS Applied Nano Materials* **2020,** *3* (1), 257-263.
43. Han, Z.; Kortlever, R.; Chen, H.-Y.; Peters, J. C.; Agapie, T., CO_2 Reduction Selective for $C_{\geq 2}$ Products on Polycrystalline Copper with N-Substituted Pyridinium Additives. *ACS Central Science* **2017,** *3* (8), 853-859.
44. Li, F.; Li, Y. C.; Wang, Z.; Li, J.; Nam, D.-H.; Lum, Y.; Luo, M.; Wang, X.; Ozden, A.; Hung, S.-F.; Chen, B.; Wang, Y.; Wicks, J.; Xu, Y.; Li, Y.; Gabardo, C. M.; Dinh, C.-T.; Wang, Y.; Zhuang, T.-T.; Sinton, D.; Sargent, E. H., Cooperative CO_2-to-ethanol conversion via enriched intermediates at molecule–metal catalyst interfaces. *Nature Catalysis* **2020,** *3* (1), 75-82.
45. Kas, R.; Kortlever, R.; Milbrat, A.; Koper, M. T. M.; Mul, G.; Baltrusaitis, J., Electrochemical CO_2 reduction on Cu_2O-derived copper nanoparticles: controlling the catalytic selectivity of hydrocarbons. *Physical Chemistry Chemical Physics* **2014,** *16* (24), 12194-12201.
46. Lum, Y.; Yue, B.; Lobaccaro, P.; Bell, A. T.; Ager, J. W., Optimizing C–C Coupling on Oxide-Derived Copper Catalysts for Electrochemical CO_2 Reduction. *The Journal of Physical Chemistry C* **2017,** *121* (26), 14191-14203.
47. Eilert, A.; Cavalca, F.; Roberts, F. S.; Osterwalder, J.; Liu, C.; Favaro, M.; Crumlin, E. J.; Ogasawara, H.; Friebel, D.; Pettersson, L. G. M.; Nilsson, A., Subsurface Oxygen in Oxide-Derived Copper Electrocatalysts for Carbon Dioxide Reduction. *The Journal of Physical Chemistry Letters* **2017,** *8* (1), 285-290.
48. Shah, A. H.; Wang, Y.; Hussain, S.; Akbar, M. B.; Woldu, A. R.; Zhang, X.; He, T., New aspects of C_2 selectivity in electrochemical CO_2 reduction over oxide-derived copper. *Physical Chemistry Chemical Physics* **2020,** *22* (4), 2046-2053.
49. Favaro, M.; Xiao, H.; Cheng, T.; Goddard, W. A., 3rd; Yano, J.; Crumlin, E. J., Subsurface oxide plays a critical role in CO_2 activation by Cu(111) surfaces to form chemisorbed CO_2, the first step in reduction of CO_2. *Proceedings of the National Academy of Sciences of the United States of America* **2017,** *114* (26), 6706-6711.
50. Xiao, H.; Goddard, W. A., 3rd; Cheng, T.; Liu, Y., Cu metal embedded in oxidized matrix catalyst to promote CO_2 activation and CO dimerization for electrochemical reduction of CO_2. *Proceedings of the National Academy of Sciences of the United States of America* **2017,** *114* (26), 6685-6688.
51. Ren, D.; Deng, Y.; Handoko, A. D.; Chen, C. S.; Malkhandi, S.; Yeo, B. S., Selective Electrochemical Reduction of Carbon Dioxide to Ethylene and Ethanol on Copper(I) Oxide Catalysts. *ACS Catalysis* **2015,** *5* (5), 2814-2821.
52. Mandal, L.; Yang, K. R.; Motapothula, M. R.; Ren, D.; Lobaccaro, P.; Patra, A.; Sherburne, M.; Batista, V. S.; Yeo, B. S.; Ager, J. W.; Martin, J.; Venkatesan, T., Investigating the Role of Copper Oxide in Electrochemical CO_2 Reduction in Real Time. *ACS Applied Materials & Interfaces* **2018,** *10* (10), 8574-8584.

53. Lum, Y.; Ager, J. W., Stability of Residual Oxides in Oxide-Derived Copper Catalysts for Electrochemical CO_2 Reduction Investigated with ^{18}O Labeling. *Angewandte Chemie International Edition* **2018,** *57* (2), 551-554.
54. Mistry, H.; Varela, A. S.; Bonifacio, C. S.; Zegkinoglou, I.; Sinev, I.; Choi, Y.-W.; Kisslinger, K.; Stach, E. A.; Yang, J. C.; Strasser, P.; Cuenya, B. R., Highly selective plasma-activated copper catalysts for carbon dioxide reduction to ethylene. *Nature Communications* **2016,** *7* (1), 12123.
55. De Luna, P.; Quintero-Bermudez, R.; Dinh, C.-T.; Ross, M. B.; Bushuyev, O. S.; Todorović, P.; Regier, T.; Kelley, S. O.; Yang, P.; Sargent, E. H., Catalyst electro-redeposition controls morphology and oxidation state for selective carbon dioxide reduction. *Nature Catalysis* **2018,** *1* (2), 103-110.
56. Yang, P.-P.; Zhang, X.-L.; Gao, F.-Y.; Zheng, Y.-R.; Niu, Z.-Z.; Yu, X.; Liu, R.; Wu, Z.-Z.; Qin, S.; Chi, L.-P.; Duan, Y.; Ma, T.; Zheng, X.-S.; Zhu, J.-F.; Wang, H.-J.; Gao, M.-R.; Yu, S.-H., Protecting Copper Oxidation State via Intermediate Confinement for Selective CO_2 Electroreduction to C_{2+} Fuels. *Journal of the American Chemical Society* **2020,** *142* (13), 6400-6408.
57. Lee, S. Y.; Jung, H.; Kim, N.-K.; Oh, H.-S.; Min, B. K.; Hwang, Y. J., Mixed Copper States in Anodized Cu Electrocatalyst for Stable and Selective Ethylene Production from CO_2 Reduction. *Journal of the American Chemical Society* **2018,** *140* (28), 8681-8689.
58. Gao, S.; Sun, Z.; Liu, W.; Jiao, X.; Zu, X.; Hu, Q.; Sun, Y.; Yao, T.; Zhang, W.; Wei, S.; Xie, Y., Atomic layer confined vacancies for atomic-level insights into carbon dioxide electroreduction. *Nature Communications* **2017,** *8* (1), 14503.
59. Daiyan, R.; Lu, X.; Saputera, W. H.; Ng, Y. H.; Amal, R., Highly Selective Reduction of CO_2 to Formate at Low Overpotentials Achieved by a Mesoporous Tin Oxide Electrocatalyst. *ACS Sustainable Chemistry & Engineering* **2018,** *6* (2), 1670-1679.
60. Kitchin, J. R.; Nørskov, J. K.; Barteau, M. A.; Chen, J. G., Role of Strain and Ligand Effects in the Modification of the Electronic and Chemical Properties of Bimetallic Surfaces. *Physical Review Letters* **2004,** *93* (15), 156801.
61. Kitchin, J. R.; Nørskov, J. K.; Barteau, M. A.; Chen, J. G., Modification of the surface electronic and chemical properties of Pt(111) by subsurface 3d transition metals. *The Journal of Chemical Physics* **2004,** *120* (21), 10240-10246.
62. Nørskov, J. K.; Bligaard, T.; Rossmeisl, J.; Christensen, C. H., Towards the computational design of solid catalysts. *Nature Chemistry* **2009,** *1* (1), 37-46.
63. Clark, E. L.; Hahn, C.; Jaramillo, T. F.; Bell, A. T., Electrochemical CO_2 Reduction over Compressively Strained CuAg Surface Alloys with Enhanced Multi-Carbon Oxygenate Selectivity. *Journal of the American Chemical Society* **2017,** *139* (44), 15848-15857.
64. Huang, J.; Mensi, M.; Oveisi, E.; Mantella, V.; Buonsanti, R., Structural Sensitivities in Bimetallic Catalysts for Electrochemical CO_2 Reduction Revealed by Ag–Cu Nanodimers. *Journal of the American Chemical Society* **2019,** *141* (6), 2490-2499.
65. Zhang, Z.; Melo, L.; Jansonius, R. P.; Habibzadeh, F.; Grant, E. R.; Berlinguette, C. P., pH Matters When Reducing CO_2 in an Electrochemical Flow Cell. *ACS Energy Letters* **2020,** *5* (10), 3101-3107.
66. Dai, L., Functionalization of Graphene for Efficient Energy Conversion and Storage. *Accounts of Chemical Research* **2013,** *46* (1), 31-42.

67. Vasileff, A.; Zheng, Y.; Qiao, S. Z., Carbon Solving Carbon's Problems: Recent Progress of Nanostructured Carbon-Based Catalysts for the Electrochemical Reduction of CO2. *Advanced Energy Materials* **2017,** *7* (21), 1700759.
68. Wang, H.; Maiyalagan, T.; Wang, X., Review on Recent Progress in Nitrogen-Doped Graphene: Synthesis, Characterization, and Its Potential Applications. *ACS Catalysis* **2012,** *2* (5), 781-794.
69. Sharma, P. P.; Wu, J.; Yadav, R. M.; Liu, M.; Wright, C. J.; Tiwary, C. S.; Yakobson, B. I.; Lou, J.; Ajayan, P. M.; Zhou, X.-D., Nitrogen-Doped Carbon Nanotube Arrays for High-Efficiency Electrochemical Reduction of CO_2: On the Understanding of Defects, Defect Density, and Selectivity. *Angewandte Chemie International Edition* **2015,** *54* (46), 13701-13705.
70. Zhang, S.; Kang, P.; Ubnoske, S.; Brennaman, M. K.; Song, N.; House, R. L.; Glass, J. T.; Meyer, T. J., Polyethylenimine-Enhanced Electrocatalytic Reduction of CO_2 to Formate at Nitrogen-Doped Carbon Nanomaterials. *Journal of the American Chemical Society* **2014,** *136* (22), 7845-7848.
71. Wu, J.; Liu, M.; Sharma, P. P.; Yadav, R. M.; Ma, L.; Yang, Y.; Zou, X.; Zhou, X.-D.; Vajtai, R.; Yakobson, B. I.; Lou, J.; Ajayan, P. M., Incorporation of Nitrogen Defects for Efficient Reduction of CO_2 via Two-Electron Pathway on Three-Dimensional Graphene Foam. *Nano Letters* **2016,** *16* (1), 466-470.
72. Chai, G.-L.; Guo, Z.-X., Highly effective sites and selectivity of nitrogen-doped graphene/CNT catalysts for CO_2 electrochemical reduction. *Chemical Science* **2016,** *7* (2), 1268-1275.
73. Hursán, D.; Janáky, C., Electrochemical Reduction of Carbon Dioxide on Nitrogen-Doped Carbons: Insights from Isotopic Labeling Studies. *ACS Energy Letters* **2018,** *3* (3), 722-723.
74. Kumar, B.; Asadi, M.; Pisasale, D.; Sinha-Ray, S.; Rosen, B. A.; Haasch, R.; Abiade, J.; Yarin, A. L.; Salehi-Khojin, A., Renewable and metal-free carbon nanofibre catalysts for carbon dioxide reduction. *Nature Communications* **2013,** *4*, 2819.
75. Wu, J.; Yadav, R. M.; Liu, M.; Sharma, P. P.; Tiwary, C. S.; Ma, L.; Zou, X.; Zhou, X.-D.; Yakobson, B. I.; Lou, J.; Ajayan, P. M., Achieving Highly Efficient, Selective, and Stable CO_2 Reduction on Nitrogen-Doped Carbon Nanotubes. *ACS Nano* **2015,** *9* (5), 5364-5371.
76. Lu, X.; Tan, T. H.; Ng, Y. H.; Amal, R., Highly Selective and Stable Reduction of CO_2 to CO by a Graphitic Carbon Nitride/Carbon Nanotube Composite Electrocatalyst. *Chemistry – A European Journal* **2016,** *22* (34), 11991-11996.
77. Wang, H.; Chen, Y.; Hou, X.; Ma, C.; Tan, T., Nitrogen-doped graphenes as efficient electrocatalysts for the selective reduction of carbon dioxide to formate in aqueous solution. *Green Chemistry* **2016,** *18* (11), 3250-3256.
78. Sun, X.; Kang, X.; Zhu, Q.; Ma, J.; Yang, G.; Liu, Z.; Han, B., Very highly efficient reduction of CO_2 to CH_4 using metal-free N-doped carbon electrodes. *Chemical Science* **2016,** *7* (4), 2883-2887.
79. Wu, J.; Ma, S.; Sun, J.; Gold, J. I.; Tiwary, C.; Kim, B.; Zhu, L.; Chopra, N.; Odeh, I. N.; Vajtai, R.; Yu, A. Z.; Luo, R.; Lou, J.; Ding, G.; Kenis, P. J. A.; Ajayan, P. M., A metal-free electrocatalyst for carbon dioxide reduction to multi-carbon hydrocarbons and oxygenates. *Nature Communications* **2016,** *7*, 13869.

80. Song, Y.; Chen, W.; Zhao, C.; Li, S.; Wei, W.; Sun, Y., Metal-Free Nitrogen-Doped Mesoporous Carbon for Electroreduction of CO_2 to Ethanol. *Angewandte Chemie International Edition* **2017,** *56* (36), 10840-10844.
81. Ju, W.; Bagger, A.; Hao, G.-P.; Varela, A. S.; Sinev, I.; Bon, V.; Roldan Cuenya, B.; Kaskel, S.; Rossmeisl, J.; Strasser, P., Understanding activity and selectivity of metal-nitrogen-doped carbon catalysts for electrochemical reduction of CO_2. *Nature Communications* **2017,** *8* (1), 944.
82. Huan, T. N.; Ranjbar, N.; Rousse, G.; Sougrati, M.; Zitolo, A.; Mougel, V.; Jaouen, F.; Fontecave, M., Electrochemical Reduction of CO_2 Catalyzed by Fe-N-C Materials: A Structure–Selectivity Study. *ACS Catalysis* **2017,** *7* (3), 1520-1525.
83. Li, X.; Bi, W.; Chen, M.; Sun, Y.; Ju, H.; Yan, W.; Zhu, J.; Wu, X.; Chu, W.; Wu, C.; Xie, Y., Exclusive Ni–N_4 Sites Realize Near-Unity CO Selectivity for Electrochemical CO_2 Reduction. *Journal of the American Chemical Society* **2017,** *139* (42), 14889-14892.
84. Hu, X.-M.; Hval, H. H.; Bjerglund, E. T.; Dalgaard, K. J.; Madsen, M. R.; Pohl, M.-M.; Welter, E.; Lamagni, P.; Buhl, K. B.; Bremholm, M.; Beller, M.; Pedersen, S. U.; Skrydstrup, T.; Daasbjerg, K., Selective CO_2 Reduction to CO in Water using Earth-Abundant Metal and Nitrogen-Doped Carbon Electrocatalysts. *ACS Catalysis* **2018,** *8* (7), 6255-6264.
85. Zhang, C.; Yang, S.; Wu, J.; Liu, M.; Yazdi, S.; Ren, M.; Sha, J.; Zhong, J.; Nie, K.; Jalilov, A. S.; Li, Z.; Li, H.; Yakobson, B. I.; Wu, Q.; Ringe, E.; Xu, H.; Ajayan, P. M.; Tour, J. M., Electrochemical CO_2 Reduction with Atomic Iron-Dispersed on Nitrogen-Doped Graphene. *Advanced Energy Materials* **2018,** *8* (19), 1703487.
86. Pan, F.; Deng, W.; Justiniano, C.; Li, Y., Identification of champion transition metals centers in metal and nitrogen-codoped carbon catalysts for CO_2 reduction. *Applied Catalysis B: Environmental* **2018,** *226*, 463-472.
87. Zhou, H.; Zou, X.; Wu, X.; Yang, X.; Li, J., Coordination Engineering in Cobalt–Nitrogen-Functionalized Materials for CO_2 Reduction. *The Journal of Physical Chemistry Letters* **2019,** *10* (21), 6551-6557.
88. Varela, A. S.; Ju, W.; Bagger, A.; Franco, P.; Rossmeisl, J.; Strasser, P., Electrochemical Reduction of CO_2 on Metal-Nitrogen-Doped Carbon Catalysts. *ACS Catalysis* **2019,** *9* (8), 7270-7284.
89. Zhu, Y.; Sokolowski, J.; Song, X.; He, Y.; Mei, Y.; Wu, G., Engineering Local Coordination Environments of Atomically Dispersed and Heteroatom-Coordinated Single Metal Site Electrocatalysts for Clean Energy-Conversion. *Advanced Energy Materials* **2020,** *10* (11), 1902844.
90. Sheridan, L. B.; Hensley, D. K.; Lavrik, N. V.; Smith, S. C.; Schwartz, V.; Liang, C.; Wu, Z.; Meyer, H. M.; Rondinone, A. J., Growth and Electrochemical Characterization of Carbon Nanospike Thin Film Electrodes. *Journal of The Electrochemical Society* **2014,** *161* (9), H558-H563.
91. Yuan, J.; Zhi, W.-Y.; Liu, L.; Yang, M.-P.; Wang, H.; Lu, J.-X., Electrochemical reduction of CO_2 at metal-free N-functionalized graphene oxide electrodes. *Electrochimica Acta* **2018,** *282*, 694-701.
92. Singh, M. R.; Kwon, Y.; Lum, Y.; Ager, J. W.; Bell, A. T., Hydrolysis of Electrolyte Cations Enhances the Electrochemical Reduction of CO_2 over Ag and Cu. *Journal of the American Chemical Society* **2016,** *138* (39), 13006-13012.

93. Xu, W.; Qiu, Y.; Zhang, T.; Li, X.; Zhang, H., The Effect of Organic Additives on the Activity and Selectivity of CO_2 Electroreduction: The Role of Functional Groups. *ChemSusChem* **2018,** *11* (17), 2904-2911.
94. Wagner, A.; Sahm, C. D.; Reisner, E., Towards molecular understanding of local chemical environment effects in electro- and photocatalytic CO_2 reduction. *Nature Catalysis* **2020,** *3* (10), 775-786.
95. Nam, D.-H.; De Luna, P.; Rosas-Hernández, A.; Thevenon, A.; Li, F.; Agapie, T.; Peters, J. C.; Shekhah, O.; Eddaoudi, M.; Sargent, E. H., Molecular enhancement of heterogeneous CO_2 reduction. *Nature Materials* **2020,** *19* (3), 266-276.
96. Kim, C.; Jeon, H. S.; Eom, T.; Jee, M. S.; Kim, H.; Friend, C. M.; Min, B. K.; Hwang, Y. J., Achieving Selective and Efficient Electrocatalytic Activity for CO_2 Reduction Using Immobilized Silver Nanoparticles. *Journal of the American Chemical Society* **2015,** *137* (43), 13844-13850.
97. Kim, C.; Eom, T.; Jee, M. S.; Jung, H.; Kim, H.; Min, B. K.; Hwang, Y. J., Insight into Electrochemical CO_2 Reduction on Surface-Molecule-Mediated Ag Nanoparticles. *ACS Catalysis* **2017,** *7* (1), 779-785.
98. Wakerley, D.; Lamaison, S.; Ozanam, F.; Menguy, N.; Mercier, D.; Marcus, P.; Fontecave, M.; Mougel, V., Bio-inspired hydrophobicity promotes CO_2 reduction on a Cu surface. *Nature Materials* **2019,** *18* (11), 1222-1227.
99. Zhao, Y.; Wang, C.; Liu, Y.; MacFarlane, D. R.; Wallace, G. G., Engineering Surface Amine Modifiers of Ultrasmall Gold Nanoparticles Supported on Reduced Graphene Oxide for Improved Electrochemical CO_2 Reduction. *Advanced Energy Materials* **2018,** *8* (25), 1801400.
100. Marjolin, A.; Keith, J. A., Thermodynamic Descriptors for Molecules That Catalyze Efficient CO_2 Electroreductions. *ACS Catalysis* **2015,** *5* (2), 1123-1130.
101. Thevenon, A.; Rosas-Hernández, A.; Peters, J. C.; Agapie, T., In-Situ Nanostructuring and Stabilization of Polycrystalline Copper by an Organic Salt Additive Promotes Electrocatalytic CO_2 Reduction to Ethylene. *Angewandte Chemie International Edition* **2019,** *58* (47), 16952-16958.
102. Li, F.; Thevenon, A.; Rosas-Hernández, A.; Wang, Z.; Li, Y.; Gabardo, C. M.; Ozden, A.; Dinh, C. T.; Li, J.; Wang, Y.; Edwards, J. P.; Xu, Y.; McCallum, C.; Tao, L.; Liang, Z.-Q.; Luo, M.; Wang, X.; Li, H.; O'Brien, C. P.; Tan, C.-S.; Nam, D.-H.; Quintero-Bermudez, R.; Zhuang, T.-T.; Li, Y. C.; Han, Z.; Britt, R. D.; Sinton, D.; Agapie, T.; Peters, J. C.; Sargent, E. H., Molecular tuning of CO_2-to-ethylene conversion. *Nature* **2020,** *577* (7791), 509-513.
103. Barton Cole, E.; Lakkaraju, P. S.; Rampulla, D. M.; Morris, A. J.; Abelev, E.; Bocarsly, A. B., Using a One-Electron Shuttle for the Multielectron Reduction of CO_2 to Methanol: Kinetic, Mechanistic, and Structural Insights. *Journal of the American Chemical Society* **2010,** *132* (33), 11539-11551.
104. Wang, X.; Wang, Z.; García de Arquer, F. P.; Dinh, C.-T.; Ozden, A.; Li, Y. C.; Nam, D.-H.; Li, J.; Liu, Y.-S.; Wicks, J.; Chen, Z.; Chi, M.; Chen, B.; Wang, Y.; Tam, J.; Howe, J. Y.; Proppe, A.; Todorović, P.; Li, F.; Zhuang, T.-T.; Gabardo, C. M.; Kirmani, A. R.; McCallum, C.; Hung, S.-F.; Lum, Y.; Luo, M.; Min, Y.; Xu, A.; O'Brien, C. P.; Stephen, B.; Sun, B.; Ip, A. H.; Richter, L. J.; Kelley, S. O.; Sinton, D.; Sargent, E. H., Efficient electrically powered CO_2-to-ethanol via suppression of deoxygenation. *Nature Energy* **2020,** *5* (6), 478-486.

105. Chen, C.; Yan, X.; Liu, S.; Wu, Y.; Wan, Q.; Sun, X.; Zhu, Q.; Liu, H.; Ma, J.; Zheng, L.; Wu, H.; Han, B., Highly Efficient Electroreduction of CO_2 to C_{2+} Alcohols on Heterogeneous Dual Active Sites. *Angew Chem Int Ed Engl* **2020,** *59* (38), 16459-16464.
106. Luo, M.; Wang, Z.; Li, Y. C.; Li, J.; Li, F.; Lum, Y.; Nam, D.-H.; Chen, B.; Wicks, J.; Xu, A.; Zhuang, T.; Leow, W. R.; Wang, X.; Dinh, C.-T.; Wang, Y.; Wang, Y.; Sinton, D.; Sargent, E. H., Hydroxide promotes carbon dioxide electroreduction to ethanol on copper via tuning of adsorbed hydrogen. *Nature Communications* **2019,** *10* (1), 5814.
107. Chen, Z.; Wang, T.; Liu, B.; Cheng, D.; Hu, C.; Zhang, G.; Zhu, W.; Wang, H.; Zhao, Z.-J.; Gong, J., Grain-Boundary-Rich Copper for Efficient Solar-Driven Electrochemical CO_2 Reduction to Ethylene and Ethanol. *Journal of the American Chemical Society* **2020,** *142* (15), 6878-6883.
108. Fan, L.; Xia, C.; Yang, F.; Wang, J.; Wang, H.; Lu, Y., Strategies in catalysts and electrolyzer design for electrochemical CO_2 reduction toward C_{2+} products. *Sci Adv* **2020,** *6* (8), eaay3111.
109. Raciti, D.; Mao, M.; Park, J. H.; Wang, C., Local pH Effect in the CO_2 Reduction Reaction on High-Surface-Area Copper Electrocatalysts. *Journal of The Electrochemical Society* **2018,** *165* (10), F799-F804.
110. Varela, A. S.; Kroschel, M.; Reier, T.; Strasser, P., Controlling the selectivity of CO_2 electroreduction on copper: The effect of the electrolyte concentration and the importance of the local pH. *Catalysis Today* **2016,** *260*, 8-13.
111. Dinh, C.-T.; Jain, A.; de Arquer, F. P. G.; De Luna, P.; Li, J.; Wang, N.; Zheng, X.; Cai, J.; Gregory, B. Z.; Voznyy, O.; Zhang, B.; Liu, M.; Sinton, D.; Crumlin, E. J.; Sargent, E. H., Multi-site electrocatalysts for hydrogen evolution in neutral media by destabilization of water molecules. *Nature Energy* **2019,** *4* (2), 107-114.
112. Xiao, H.; Cheng, T.; Goddard, W. A., Atomistic Mechanisms Underlying Selectivities in C_1 and C_2 Products from Electrochemical Reduction of CO on Cu(111). *Journal of the American Chemical Society* **2017,** *139* (1), 130-136.
113. Lum, Y.; Cheng, T.; Goddard, W. A.; Ager, J. W., Electrochemical CO Reduction Builds Solvent Water into Oxygenate Products. *Journal of the American Chemical Society* **2018,** *140* (30), 9337-9340.
114. Feng, X.; Jiang, K.; Fan, S.; Kanan, M. W., Grain-Boundary-Dependent CO_2 Electroreduction Activity. *Journal of the American Chemical Society* **2015,** *137* (14), 4606-4609.
115. Feng, X.; Jiang, K.; Fan, S.; Kanan, M. W., A Direct Grain-Boundary-Activity Correlation for CO Electroreduction on Cu Nanoparticles. *ACS Central Science* **2016,** *2* (3), 169-174.
116. Kim, Y.; Park, S.; Shin, S.-J.; Choi, W.; Min, B. K.; Kim, H.; Kim, W.; Hwang, Y. J., Time-resolved observation of C–C coupling intermediates on Cu electrodes for selective electrochemical CO_2 reduction. *Energy & Environmental Science* **2020,** *13* (11), 4301-4311.
117. Piqué, O.; Viñes, F.; Illas, F.; Calle-Vallejo, F., Elucidating the Structure of Ethanol-Producing Active Sites at Oxide-Derived Cu Electrocatalysts. *ACS Catalysis* **2020,** *10* (18), 10488-10494.
118. Jiao, Y.; Zheng, Y.; Chen, P.; Jaroniec, M.; Qiao, S.-Z., Molecular Scaffolding Strategy with Synergistic Active Centers To Facilitate Electrocatalytic CO_2 Reduction to

Hydrocarbon/Alcohol. *Journal of the American Chemical Society* **2017,** *139* (49), 18093-18100.